Postprint of: Kwiatkowski A., Drozdowska K., Smulko J., Embedded gas sensing setup for air samples analysis, REVIEW OF SCIENTIFIC INSTRUMENTS, Vol. 92, iss. 7 (2021), 074102, DOI: 10.1063/5.0050445

Embedded gas sensing set-up for air samples analysis

Andrzej Kwiatkowski[a)], Katarzyna Drozdowska, Janusz Smulko

Faculty of Electronics, Telecommunications and Informatics, and Digital Technologies Center, Gdańsk University of Technology, Narutowicza 11/12, 80-233 Gdańsk, Poland

[a)]Author to whom correspondence should be addressed: andrzej.kwiatkowski@pg.edu.pl

Abstract

This paper describes a measurement set-up (eNose) designed to analyse air samples containing various volatile organic compounds (VOCs). The set-up utilises a set of resistive gas sensors of divergent gas selectivity and sensitivity. Some of the applied sensors are commercially available and were proposed recently to reduce their consumed energy. The sensors detect various VOCs at sensitivities determined by metal oxide sensors technology and operating conditions. The set-up can utilise prototype gas sensors, made of resistive layers of different compositions, as well. Their properties can be modulated by selecting operating temperature or using UV light irradiation. The unit is controlled by an embedded system M5Stack Core2 ESP32 IoT. We used this development kit to program the measurement procedure and data recording fastly. The set-up utilises an aluminium gas chamber of a volume of 220 ml, a set of electrical valves to introduce there an air sample with the help of an electrical micropump. The handling of the set-up was simplified to a selection of a few operations by touch screen only without a necessity of extra training. The recorded data are saved in a memory card for further processing. The evolved set-up can be upgraded to apply more advanced data processing by utilising WiFi or Bluetooth connection. The control program was prepared using the Arduino IDE software environment and can be further advanced with ease. The applied materials and the established measurement procedure can use various air samples, including exhaled breath samples for patients screening check-ups. We applied the same time of 10 min. for response and recovery, acceptable for practical use.

1. Introduction

Gas analysis attracts the attention of numerous research groups because of its high practical impact and a need for further improvements.[1,2] Various methods and technologies are utilised to detect gaseous compounds.[3] Even greater attention focuses on the determination of volatile organic compounds (VOCs) due to their toxic effects and potential application in the food industry (e.g., detection of bioagents emitted by bacteria, moulds and fungi) or medical check-ups (e.g., exhaled breath analysis).[4] Resistive gas sensors are attractive sensors of relatively long-time durability and acceptable sensitivity.[5] Metal oxide semiconductors (MOX – e.g., SnO_2, WO_3, TiO_2) are used for their construction. An application of selected dopants improves their selectivity and sensitivity.[6]

The response of resistive gas sensors to ambient gases can be determined by recording their DC resistances using a simple electronic circuit.[7,8] The sensors are characterised by the same response to different gases and therefore cannot be applied for determining the components of gas mixtures as an individual sensor. Thus, we comprise an array of gas sensors with different but overlapping selectivity and sensitivity. Such devices are still developed and popularised even in everyday devices like smartphones due to technological advances.[9,10] The responses of the resistive sensors form a data vector which is further processed by various algorithms.[11] We propose to record DC resistances changes after injecting the gas sample into the gas chamber until the resistances of the sensors stabilise.

Various methods are applied to enhance the gas sensing of the MOX sensors. UV light irradiation enhances gas sensing in the sensing layers exhibiting photocatalytic effect (e.g., WO_3, TiO_2, ZnO).[12,13] It improves sensitivity at low gas concentrations and improves detection level.[14] Another way of improving gas sensing utilises low-frequency resistance fluctuations.[15,16] The last method requires a more precise measurement set-up to record noise data at a low-frequency range but can ensure much better gas sensitivity. The issues of improving gas sensitivity by the gas sensors and using various methods (e.g., surface acoustic wave – SAW, quartz crystal microbalance – QCM)[17], materials (e.g., two-dimensional materials and nanostructures, functionalized at atomic scale nanomaterials)[18,19] were investigated by different research teams.

Another popular and commercially available gas sensors are the electrochemical sensors. The sensors are bulkier than the recently developed MOX sensors but do not require much heating energy. Their output signal is a voltage signal and can be easily recorded in an electronic measurement set-up. Electrochemical sensors can be characterised by similar durability as the MOX sensors and limited gas selectivity.

The measurements of the above-mentioned gas sensors can be implemented in a measurement set-up and give more information about the examined gas sample. The set-up requires a microcontroller, analogue-to-digital converters (ADCs) to measure DC resistances and storage the recorded data in the files. Moreover, it has to control the operation of a few gas sensors and their heaters. The set-up has to control the valves and a micropump to clean the gas chamber at the beginning of the measurement cycle and introduce the gas sample.

There is a market for an embedded gas sensing system that can be applied for environmental monitoring or even for presenting medical applications. The system should comprise of a set of commercial gas sensors and should have the ability to process the recorded data. The

prepared measurement unit was controlled by an embedded hardware system M5Stack Core2 ESP32 IoT. The selected unit is a modularised stacking system that can be easily programmed and further developed by additional modules if necessary.

2. Measurement set-up

The developed measurement set-up utilised commonly available electronic units to establish selected operating conditions for the used gas sensors. We prepared the designed set-up to analyse air samples or exhaled breath samples collected in a plastic bag (e.g., FlexFoil PLUS Sample Bags; SKC Ltd., Dorset, UK) or in a breath sampler (e.g., BioVOC^{TM}; Makers International Ltd, Llantrisant, UK). This aim determined a selection of gas sensors sensitive to a wide range of VOCs and air pollutants. Such sensors are offered on the market due to numerous air quality monitoring applications (indoor and outdoor). Some selected data of the applied gas sensors are presented in table 1.

TABLE 1. The list of the applied commercial gas sensors of different gas selectivity and environmental monitoring conditions. The detailed descriptions of the enumerated sensors are available at the web pages of their producers: *Winsen* www.winsen-sensor.com; *Figaro* www.figarosensor.com; *SGX Sensortech* www.sgxsensortech.com; *Bosch Sensortec* www.bosch-sensortec.com.

Gas sensor	Producer	Detected gases
GM-402B	Winsen	C_3H_8,CH_4
GM-502B	Winsen	CH_2O, C_2H_5OH, C_7H_8
TGS8100	Figaro	H_2, CO, CH_4, C_2H_5OH
MiCS-6814	SGX Sensortech	CO, NH_3, NO_x, C_2H_5OH, C_3H_8, C_4H_{10}
ZE08-CH_2O (electrochemical gas sensor)	Winsen	CH_2O
BME680	Bosch Sensortec	VOCs, (temperature, humidity, pressure)

The construction of the applied MOX sensors is optimised to reduce their energy consumption, necessary for heating the gas sensing layers to accelerate the adsorption-desorption process and enhance gas sensitivity, present at elevated temperatures. The sensors require tens of mA for the heaters at maximum and can be applied even in smartphones to monitor air pollutants. The used sensor MiCS-6814 comprises three sensors sensitive to different gasses (CO, NH_3 and NO_x).

We utilised an electrochemical gas sensor (ZE08-CH_2O – TAB. 1). The separate sensor BME680 was dedicated to monitoring environmental conditions (temperature, pressure and humidity) during the measurements. These parameters have an impact on the response of the gas sensors and should be considered to evaluate the quality of the recorded data. Information about environmental conditions can exclude eventual outliers during the measurement but can also be used to enhance detection results as reported elsewhere for such systems.[20] The sensor BME680 can monitor VOCs as well and has a digital output. Some of the applied sensors (ZE08-CH_2O; BME680) have digital outputs using I^2C and UART interfaces. All necessary

calibration and DC resistances are transformed into digital numbers by the sensor chip's microcontroller. These operations are beneficial for the set-up because we can operate more sensors simultaneously by the selected embedded supervisory system M5Stack Core2 ESP32 IoT. Moreover, an application of the sensors with digital output gives a possibility to advance further the developed set-up by adding more sensors of other gas detection characteristics.

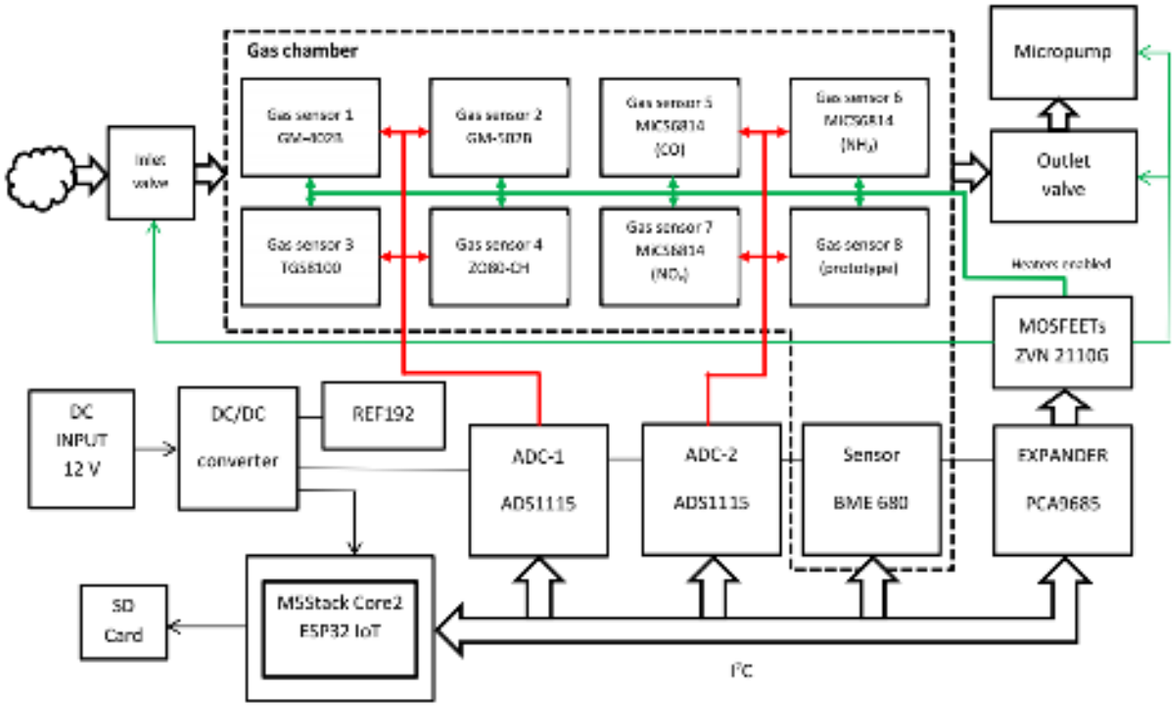

FIG. 1. Schematic diagram of the developed eNose measurement set-up.

FIGURE 1 presents the block diagram of the developed gas sensing set-up. The measurement set-up utilises commercial elements and can be easily replicated by others. The main component of the eNose set-up is the gas sensing chamber made of aluminium. Its empty volume is 220 ml. A chamber is a place for gas sensors mounted on the PCB board (FIG. 2a). We cleaned the PCB board after mounting electronic elements with isopropanol. An odourless silicone seal established the tightness of the chamber. We applied a set of the gas sensors available in the six integrated circuits and enumerated them in the TAB. 1. The developed set-up included a socket for a prototype gas sensor encased in the TO-8 sub-mount. Various prototype gas sensors of enhanced gas sensing can be used there. The set-up controlled the heater and a UV LED, emitting maximal optical power irradiation at 275 nm. These conditions enabled the application of various prototype gas sensors made of photocatalytic layers (e.g., WO_3,[21] TiO_2,[22] and NiO[23]). Such sensors, due to the applied UV irradiation, can be more sensitive to selected VOCs. Unfortunately, the prototype constructions are not optimised to minimise energy consumption for heating. Therefore, the prepared set-up uses only up to one such sensor to avoid excessive heat emission within the gas chamber.

The gas sensors responses were recorded using the I^2C interface (the sensor BME680) or by the output voltage measurements using two analogue-to-digital 16-bits converters ADS1115 (ADC-1, ADC-2 – FIG. 1). We applied a precision bandgap voltage references of 2.5V

(REF192; Analog Devices) to supply voltage dividers used for the determination of sensors DC resistances (FIG. 2a). It is a stable, low-noise reference voltage source. We provided the voltage source by 5 V using the DC/DC converter from the supplied 12 V. The resistors applied for voltage dividers were selected individually at 1% accuracy for the applied sensors exemplars due to the wide range of their DC resistances caused by the gas sensing technology.

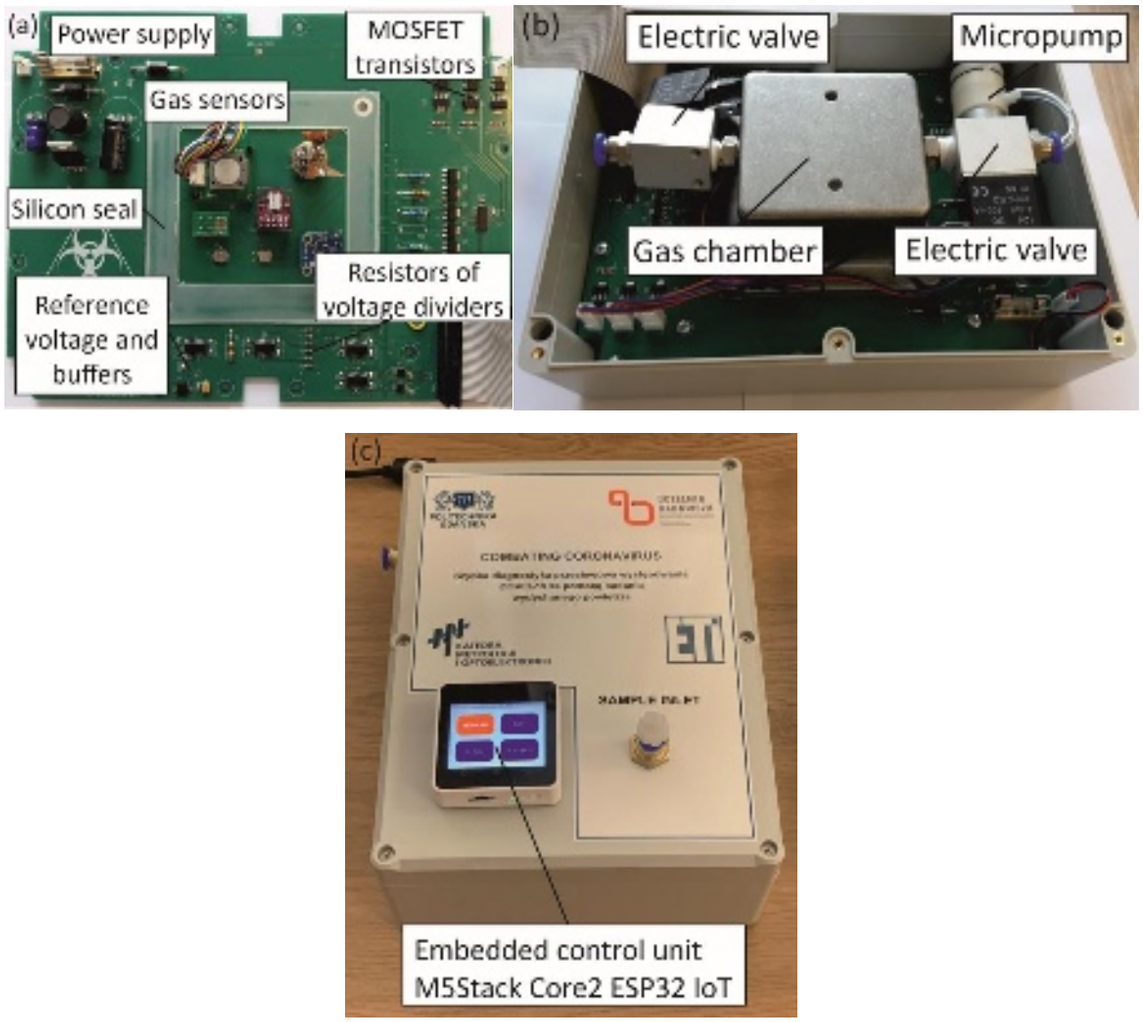

FIG. 2. Photos of the developed eNose measurement set-up: (a) PCB board with the electronic elements, (b) the mounted aluminium gas chamber, (c) the set-up ready for the measurements with the visible embedded control unit.

The expander of the I^2C interface (PCA9685; NXP) controls the MOSFET transistors (ZVN 2110G, n-type channel; DIODES Incorporated) used for regulating the heaters of the connected sensors, electric valves and a micropump (FIG. 1). These elements were controlled by the signals with pulse width modulation (PWM) of switching frequency much higher (up to 1.5 kHz) than the recorded data (at 1 Hz) to avoid eventual interferences. The MOSFETs switch on the ground of the system to the sensors heaters.

The gas chamber was designed with two independent voltage-controlled valves (FIG. 2b) at both inlet and outlet openings. A micropump, mounted at the outlet opening, was used to

make an underpressure of about 0.4 bar in the gas chamber. When the air sample is coupled to the inlet opening (sample input – Fig. 2c), the inlet valve's opening sucked the air sample into the vacuum chamber. The set-up registered the responses of the sensors after closing the inlet valve. We can set the registration time in the program parameters of the control unit.

The detailed measurements procedures were programmed by utilising the embedded system M5Stack Core2 ESP32 IoT (FIG. 2c). The device is based on dual-core 32-bit 240 MHz LX6 Xtensa® processors and is used in measurement set-ups to control the sets of sensors and actuators.[24,25] It can be connected to other devices by Bluetooth or WiFi networks. The unit can save and transmit the recorded data even on time when the sensors do not require too fast sampling. We assumed in the developed set-up to sample gas sensors responses at an arbitrarily selected sampling frequency of 1 Hz. The transmitted data can be used for computing-demand processing by selected detection algorithms using cloud server and computing centre. It has a touch screen and can be easily programmed in a few software packages independent of the level of programming skills. The system controls the measurement stages and records the sensors' responses into a file (CSV format) using SD memory card. We used 8 GB memory card, which is sufficient for the collected data. A single measurement cycle of all the connected sensors requires less than 0.2 MB of data memory for the samples saved in CSV file format.

The block diagram of the control software for the applied measurement procedure presents FIG. 3. The procedure starts with an opening CSV file and recording header information, including the selected parameters of the eNose. This phase proposes the name of the file related to a timestamp of the measurement. It means that any detailed data of the studied air sample have to be saved separately and related to the file name established by the set-up. It secures anonymity of the investigated air samples which descriptive data are saved out of the set-up. The measurements initiate the electrical valves' opening and a flow of laboratory air to clean the sensors. The micropump had a flow rate of 2-3 sccm. It means that the gas chamber (220 ml) replaced its atmosphere with the introduced laboratory air a few times within a minute. The gas chamber inlet (FIG. 2c) can be attached to a source of synthetic air if required. We can select the period of cleaning the gas chamber before the actual measurement in the set-up. The recorded exemplary data suggest that we should switch on the unit for about 30 min. and clean the gas chamber for 5 min. to get repeatable results.

Next, we closed the input valve and opened the output valve, and created a vacuum by a micropump (vacuum procedure – FIG. 3). The bag with the examined air sample (docking procedure) was then introduced into the gas chamber after opening the input valve and closing the output valve (sampling procedure). We initiated the actual measurement at this moment (measurement procedure). This procedure took 10 min. We selected this period arbitrarily to reach saturated responses (DC resistances) by most applied gas sensors. Finally, we cleaned the gas chamber again for 5 min. by introducing the air through the sample inlet (FIG. 2c). The sensors responses were continuously recorded when starting the gas chamber cleaning before the actual measurement (when the air sample was introduced into the gas chamber) and continued until the gas chamber finished the cleaning procedure. We recorded about 1200 samples for each sensor (20 min. x 60 samples = 1200).

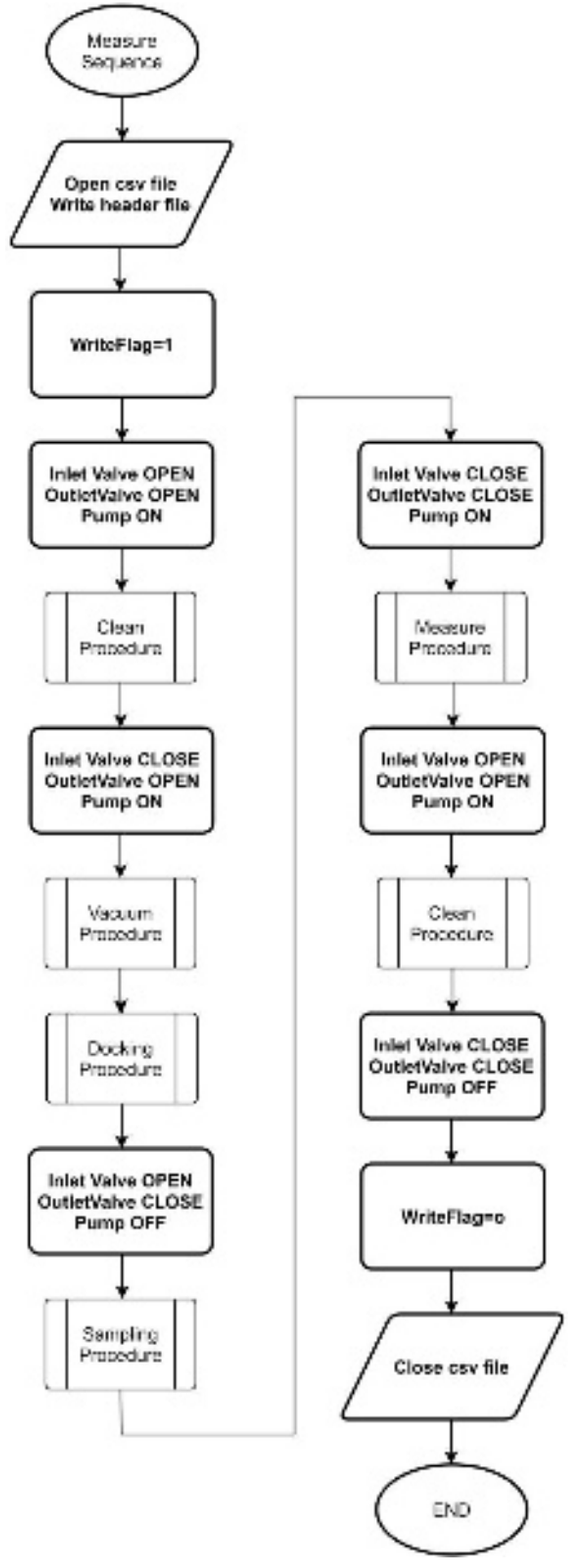

FIG. 3. Block diagram of the software controlling the measurement set-up.

The prepared software includes more modules determining the applied parameters (e.g., measurement time, sampling frequency, etc.). The supplementary information presents a more detailed description of other software modules. It is worth mentioning that the prepared

software controlled plain measurement procedures, limited to switching on and off the valves, the micropump, and recording the sensors' responses. We did not use a wireless connection to the Internet servers and eventual computing of detection algorithms. These features can be easily developed in upgraded versions of the software. We underline that the optimal selection of a detection algorithm for gas sensing is an open question.[26,27] There are some general rules of gas sensors data processing, giving acceptable detection results.[28] Unfortunately, due to gas sensors' various technologies, their drawback features related to the same response to different components of gas mixtures or humidity, we cannot propose the same universal algorithm. Still, we can use the methods of accepted computational complexity.[29,30] The recorded responses of the MOX sensors should consider not only the DC resistance at stable conditions. The sensor response comprises a few phases of characteristic shape, which can be parametrised and used as input data for the detection algorithm. Any additional information hidden in these parameters increases the efficiency of the applied algorithm. The presented eNose unit utilises mainly commercial MOX gas sensors. The same type of sensors can have even ten times different DC resistances due to variation of technology. Therefore, any measurement set-up requires calibration and selection of the resistors applied in voltage dividers to determine accurately DC resistances of the used sensors by analogue-to-digital converters of limited resolution.

3. Experimental results

We produced two copies of the same unit. One unit included an additional prototype sensor, made of NiO gas sensing layer, heated to 120 °C. Its heater elevated the temperature within the gas chamber by about an extra 3 °C when compared with the second unit.

The units were tested by applying selected air samples, including calibrating gases (C_3H_6O, NO_2) and exhaled breath. All gas samples were introduced by the sample inlet (FIG. 2c). FIGURE 4 shows the plot of relative sensors responses to a sample of acetone (30 ppm) diluted in synthetic air. The responses were recorded for both units. Sensors of the same type, but applied within two different units exhibit significant differences in DC resistances due to their technological variation. Therefore, we present relative changes in their DC resistances to compare their behaviour. It means that the proposed set-ups require calibration when selected gases are detected. The more complicated case is the detection of gas mixtures components when crossing gases induce a non-linear response of the sensors. Our units apply various algorithms and therefore can be used for detecting the presence of gas mixtures characteristic for considered illnesses or qualified as polluting gases.

The exemplary results exhibited similar shapes and intensities of the recorded changes during the measurement procedure. The sensor GM-502B had the most different resistances between the units, and this fact induced lower accuracy of DC resistance measurement for one unit (FIG. 4a). Visible differences between the units at times before the sample injection into the gas chamber resulted from a longer docking in the unit without the prototype sensor (FIG. 4a). This problem can be fixed during the measurements by keeping a similar docking time. The abrupt changes of sensors DC resistances were observed just after an air sample injection, which slowly stabilised. The stabilisation time depended on the sensor type but usually did not exceed 500 s.

One of the severe plagues of the MOX sensors is their drift during exploitation. The drift is a slow change of DC resistance induced by the sensor's structural changes (e.g., ageing, poisoning) or environmental changes (e.g., humidity, temperature).[31] It can be reduced by considering changes, or even relative changes, of sensor DC resistance. Another method requires normalisation of the sensor response versus time by examining its characteristic for calibrating gas. This approach gives better results, but we had to run periodically reference measurements.[32] Therefore, we propose the first approach to consider the relative parameters to assess the prepared eNose units. The recorded data can determine:

- the maximum value of the relative DC resistance change,
- the slope of the relative DC resistance change within selected time after air sample injection,
- relative change of DC resistance at its stabilisation at the end of the measurement procedure,
- the area under the curve presenting relative changes of DC resistance during the measurement procedure.

It is difficult to determine which of the mentioned parameters are the most informative. The answer to this question specifies the selected detection algorithm. We underline that the developed eNose set-ups exhibit some differences due to sensors technology variation, but the detection algorithm should eliminate these discrepancies using the proposed parameters. It is a unit that we can further advance by controlling the repeatability of air sample introduction and temperature stabilisation of the gas chamber.

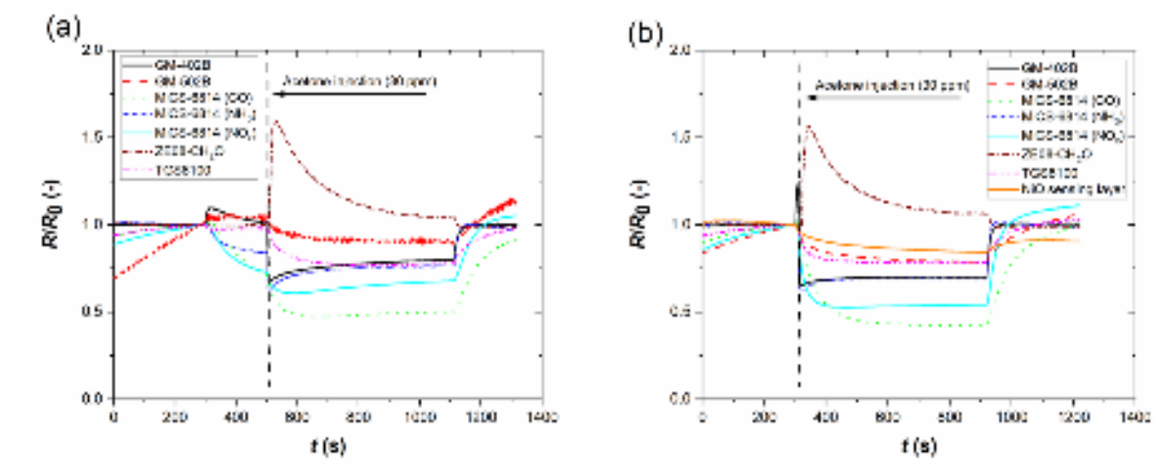

FIG. 4. Exemplary responses of the gas sensors DC resistance R at the ambient atmosphere of 30 ppm acetone (C_3H_6O) diluted in synthetic air, and observed in two available set-ups: (a) the unit comprising of six gas sensing chips – TAB. 1, (b) the unit with additional prototype gas sensing layer made of NiO nanoparticles. The data are related to DC resistance R_0 observed at time t = 500 s.

FIGURE 5 presents the selected eNose unit (with a prototype NiO gas sensor) after introducing the exhaled breath sample. Exemplary results of two volunteers (#1 and #2) collected at the same time, about 9:00 AM after fasting overnight, were selected. The last stage of exhaled breath was introduced into the gas chamber by an inlet sample. The results

show relative changes in DC resistances of the gas sensor GM-402B. We observed a clear difference in DC resistances for #1 and #2 data, exceeding 25% between their initial values (FIG. 5a). The DC resistances reached their stable values quite shortly after the sample injection.

The sensor BME680 recorded environmental conditions in the gas chamber at the same time. We observed relative differences in humidity, temperature and pressure in the gas chamber between the investigated samples of volunteers #1 and #2. Humidity varied the most between the volunteers, but the difference did not exceed 8% (FIG. 5b). Other environmental parameters (temperature – FIG. 5c; pressure – FIG. 5d) behaved in the same way for both volunteers, and the difference between #1 and #2 time series was less than 1%. It means that the recorded changes of DC resistances (sensor GM-402B) were induced mainly by differences in the exhaled breath composition than by the variation in environmental conditions between the consecutive experiments. It means that we can effectively use the set-up to analyse exhaled breath. Transferring the breath sample in the eNose by the sampler makes the procedure protective against infection between the users.

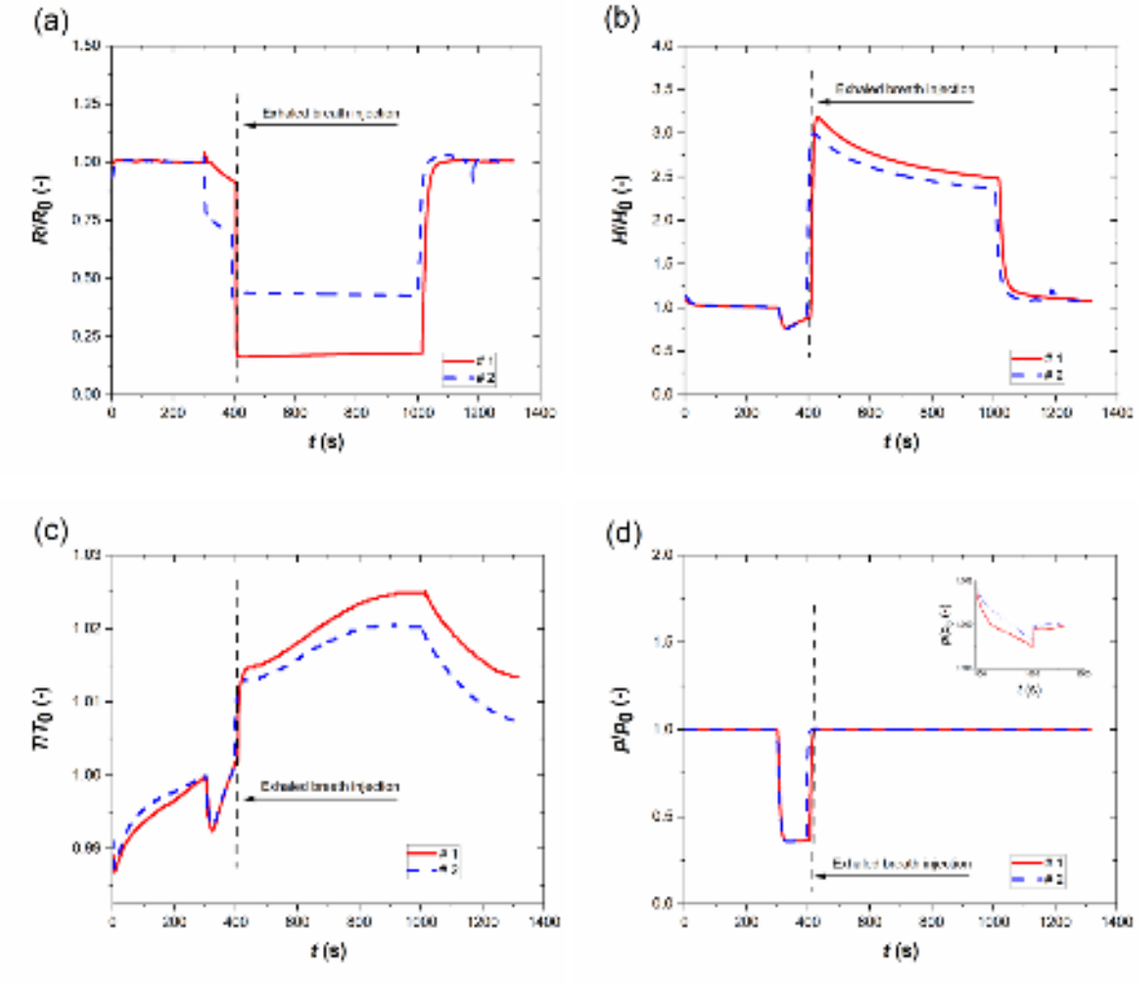

FIG. 5. The relative responses of two exemplary exhaled breath samples #1, #2: (a) DC resistance R of the gas sensor GM-402B; (b) relative humidity H, (c) temperature T [°C] and (d) pressure p [hPa] measured by the sensor BME680. The recorded data were related to their values observed at arbitrarily selected time t = 300 s, and marked with the subscript "0".

4. Conclusions

We presented in detail an eNose device utilising a set of commercial gas sensors of relatively low power consumption for their heating. The set-up monitors environmental conditions simultaneously and can apply a prototype resistive gas sensor requiring more power for heating than the commercial sensors. The eNose set-up is controlled by the embedded system by touch screen and can be further developed by introducing wireless data transmission and computing for data classification.

We demonstrated the potential of brief exhaled breath analysis with the presented unit, which can be copied and used more thoroughly. The eNose unit could work well under real-life conditions in the laboratory room. The set-up detects variations in exhaled breath composition. It can be potentially supportive for diagnosing the group of patients showing all symptoms of Covid-19 infection but not confirmed by other Covid-19 tests. It can path the way to a non-invasive detection method of virus infections. Moreover, it mainly utilizes commercial gas sensors of relatively long durability and therefore can be easily implemented when compared with other similar devices and tests for screening medical checkups.[4,33] The set-up can be also used to determine VOCs in the environment but requires cleaning the gas chamber with synthetic air instead of laboratory air used for exhaled breath samples and reducing the background effect of the inhaled air.

Supplementary material

The supplementary material includes additional figures presenting the exemplary data of selected gas sensors responses and environmental conditions recorded during the measurements. A more detailed description of the prepared software for measurements was included by presenting their block diagrams. The electronic unit applied for DC resistance measurements was also incorporated.

Author contributions

AK contributed eNose set-up design and practice; KD contributed exemplary measurements and figures preparation; JS contributed funds supporting, manuscript writing and work coordination.

Acknowledgements

Financial support of these studies from Gdańsk University of Technology by the DEC-6/2020/IDUB/I.3/CC grant under the COMBATING CORONAVIRUS – 'Excellence Initiative – Research University' program is gratefully acknowledged.

Data Availability Statement

The data that support the findings of this study are available from the corresponding author upon reasonable request.

References

1. Oluwasanya, P. W., Alzahrani, A., Kumar, V., Samad, Y. A. & Occhipinti, L. G. Portable multi-sensor air quality monitoring platform for personal exposure studies. *IEEE Instrum. Meas. Mag.* **22**, 36–44 (2019).

2. Liu, X. *et al.* A survey on gas sensing technology. *Sensors (Switzerland)* **12**, 9635–9665 (2012).

3. Korotcenkov, G. & Cho, B. K. Metal oxide composites in conductometric gas sensors: Achievements and challenges. *Sensors Actuators, B Chem.* **244**, 182–210 (2017).

4. Shan, B. *et al.* Multiplexed Nanomaterial-Based Sensor Array for Detection of COVID-19 in Exhaled Breath. *ACS Nano* (2020). doi:10.1021/acsnano.0c05657

5. Korotcenkov, G. & Cho, B. K. Engineering approaches for the improvement of conductometric gas sensor parameters: Part 1. Improvement of sensor sensitivity and selectivity (short survey). *Sensors and Actuators, B: Chemical* (2013). doi:10.1016/j.snb.2013.07.101

6. Bouchikhi, B., Chludzi, T., Saidi, T., Smulko, J. & El, N. Sensors and Actuators B : Chemical Formaldehyde detection with chemical gas sensors based on WO 3 nanowires decorated with metal nanoparticles under dark conditions and UV light irradiation. **320**, (2020).

7. Tiele, A., Wicaksono, A., Ayyala, S. K. & Covington, J. A. Development of a Compact, IoT-Enabled Electronic Nose for Breath Analysis. *Electronics* **9**, 84 (2020).

8. Arroyo, P. *et al.* Electronic Nose with Digital Gas Sensors Connected via Bluetooth to a Smartphone for Air Quality Measurements. *Sensors* **20**, 786 (2020).

9. Jaeschke, C. *et al.* An Innovative Modular eNose System Based on a Unique Combination of Analog and Digital Metal Oxide Sensors. *ACS Sensors* **4**, 2277–2281 (2019).

10. Wasilewski, T., Gębicki, J. & Kamysz, W. Bioelectronic nose: Current status and perspectives. *Biosens. Bioelectron.* **87**, 480–494 (2017).

11. Gutierrez-Osuna, R. Pattern analysis for machine olfaction: A review. *IEEE Sens. J.* **2**, 189–202 (2002).

12. Fan, S. W., Srivastava, A. K. & Dravid, V. P. UV-activated room-temperature gas sensing mechanism of polycrystalline ZnO. *Appl. Phys. Lett.* **95**, 1–4 (2009).

13. Trawka, M. *et al.* Fluctuation enhanced gas sensing with WO_3-based nanoparticle gas sensors modulated by UV light at selected wavelengths. *Sensors Actuators B Chem.* **234**, 453–461 (2016).

14. Chen, G., Paronyan, T. M., Pigos, E. M. & Harutyunyan, A. R. Enhanced gas sensing in pristine carbon nanotubes under continuous ultraviolet light illumination. *Sci. Rep.* **2**, 1–7 (2012).

15. Kish, L. B. B., Vajtai, R. & Granqvist, C. G. G. Extracting information from noise spectra of chemical sensors: single sensor electronic noses and tongues. *Sensors and Actuators B-Chemical* **71**, 55–59 (2000).

16. Ederth, J., Smulko, J. M., Kish, L. B., Heszler, P. & Granqvist, C. G. Comparison of classical and fluctuation-enhanced gas sensing with PdxWO3 nanoparticle films. *Sensors and Actuators B-Chemical* **113**, 310–315 (2006).

17. Zhang, J., Liu, X., Neri, G. & Pinna, N. Nanostructured Materials for Room-Temperature Gas Sensors. *Advanced Materials* **28**, 795–831 (2016).

18. Joshi, N. *et al.* A review on chemiresistive room temperature gas sensors based on metal oxide nanostructures, graphene and 2D transition metal dichalcogenides. *Microchim. Acta* **185**, (2018).

19. Malik, R., Tomer, V. K., Mishra, Y. K. & Lin, L. Functional gas sensing nanomaterials: A panoramic view. *Applied Physics Reviews* **7**, 21301 (2020).

20. Webster, J. *et al.* TruffleBot: Low-Cost Multi-Parametric Machine Olfaction. *2018 IEEE Biomed. Circuits Syst. Conf. BioCAS 2018 - Proc.* (2018). doi:10.1109/BIOCAS.2018.8584767

21. Bouchikhi, B. *et al.* Formaldehyde detection with chemical gas sensors based on WO3 nanowires decorated with metal nanoparticles under dark conditions and UV light irradiation. *Sensors Actuators, B Chem.* **320**, (2020).

22. Topalian, Z., Smulko, J. M., Niklasson, G. A. & Granqvist, G. G. Resistance noise in TiO2-based thin film gas sensors under ultraviolet irradiation. *J. Phys. Conf. Ser.* **76**, (2007).

23. Geng, X. *et al.* Visible light enhanced black NiO sensors for ppb-level NO_2 detection at room temperature. *Ceram. Int.* **45**, 4253–4261 (2019).

24. Villoro, A. *et al.* A TDR wireless device for volumetric water content sensing. *Comput. Electron. Agric.* **181**, 3–6 (2021).

25. Adi, P. D. P., Kitagawa, A. & Akita, J. Finger Robotic control use M5Stack board and MQTT Protocol based. *7th Int. Conf. Inf. Technol. Comput. Electr. Eng. ICITACEE 2020 - Proc.* 1–6 (2020). doi:10.1109/ICITACEE50144.2020.9239170

26. Wang, T. *et al.* A Review on Graphene-Based Gas/Vapor Sensors with Unique Properties and Potential Applications. *Nano-Micro Lett.* **8**, 95–119 (2016).

27. Mingesz, R. *et al.* Compact USB measurement and analysis system for real-time fluctuation enhanced sensing. in *Proceedings of the IEEE 21st International Conference on Noise and Fluctuations, ICNF 2011* (2011). doi:10.1109/ICNF.2011.5994350

28. Dymerski, T. M., Chmiel, T. M. & Wardencki, W. Invited Review Article: An odor-sensing system-powerful technique for foodstuff studies. *Review of Scientific Instruments* (2011). doi:10.1063/1.3660805

29. Feng, S. *et al.* Review on Smart Gas Sensing Technology. *Sensors* **19**, 3760 (2019).

30. Kalinowski, P., Woźniak, Ł., Strzelczyk, A., Jasinski, P., Jasinski, G. Efficiency of linear and non-linear classifiers for gas identification from electrocatalytic gas sensor. *Metrol. Meas. Syst.* **XX**, 501–512 (2013).

31. Vergara, A. *et al.* Chemical gas sensor drift compensation using classifier ensembles. *Sensors Actuators, B Chem.* **166**–**167**, 320–329 (2012).

32. Gardner, J. W. & Persaud, K. C. Drift reduction for metal-oxide sensor arrays using canonical correlation regression and partial least squares. *Electron. Noses Olfaction 2000* 157–162 (2020). doi:10.1201/9781482268904-29

33. Giovannini, G., Haick, H. & Garoli, D. Detecting COVID-19 from Breath: A Game Changer for a Big Challenge. *ACS Sensors* (2021). doi:10.1021/acssensors.1c00312

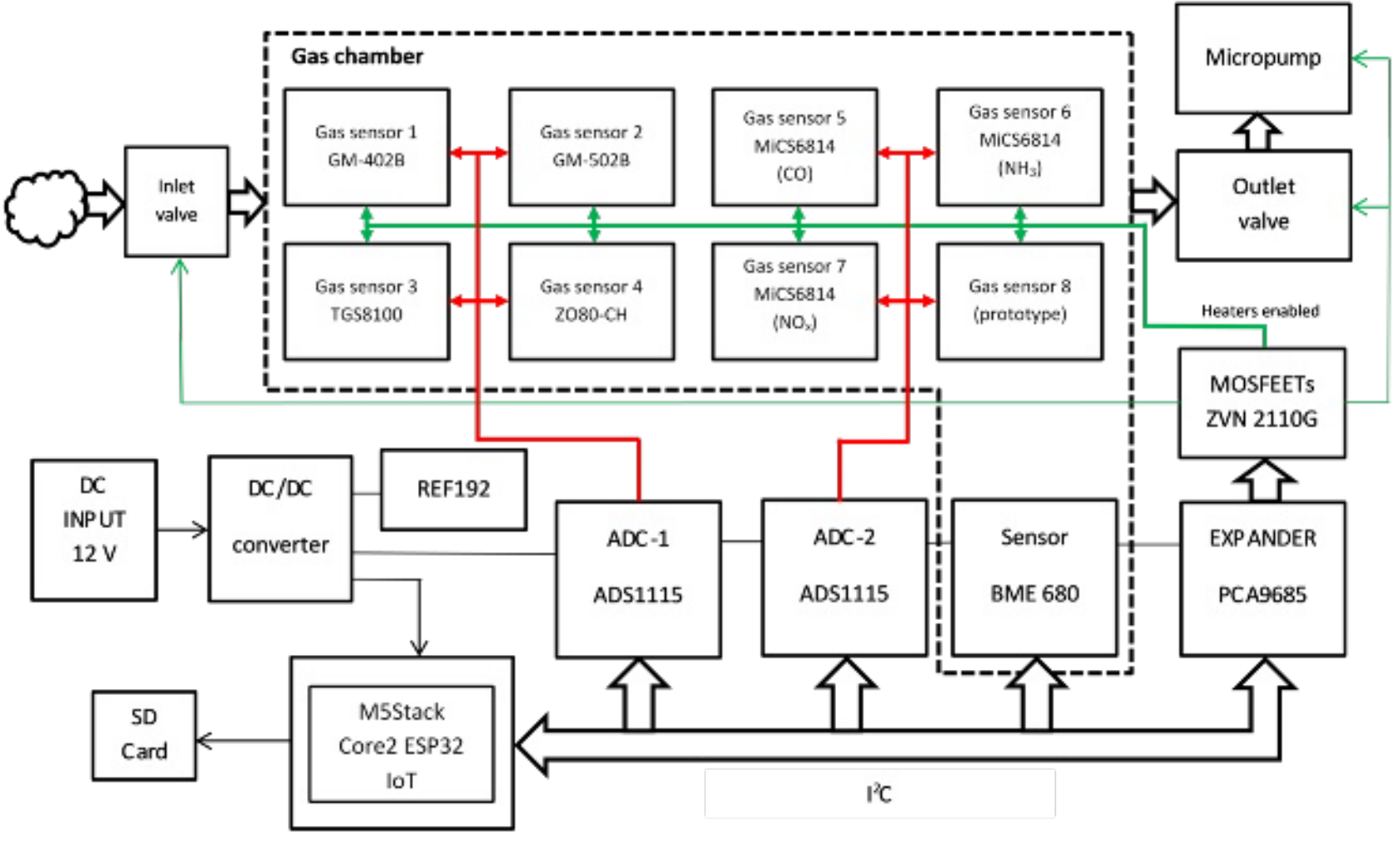
Gas chamber
Gas sensor 1
GM-402B
Gas sensor 2
GM-502B
Gas sensor 5
MICS6814
(CO)
Gas sensor 6
MICS6814
(NH3)
Gas sensor 3
TGS8100
Gas sensor 4
ZO80-CH
Gas sensor 7
MICS6814
(NOx)
Gas sensor 8
(prototype)
Inlet
valve
Micropump
Outlet
valve
Heaters enabled
MOSFEETs
ZVN 2110G
DC
INPUT
12 V
DC/DC
converter
REF192
ADC-1
ADS1115
ADC-2
ADS1115
Sensor
BME 680
EXPANDER
PCA9685
SD
Card
M5Stack
Core2 ESP32
IoT
I²C

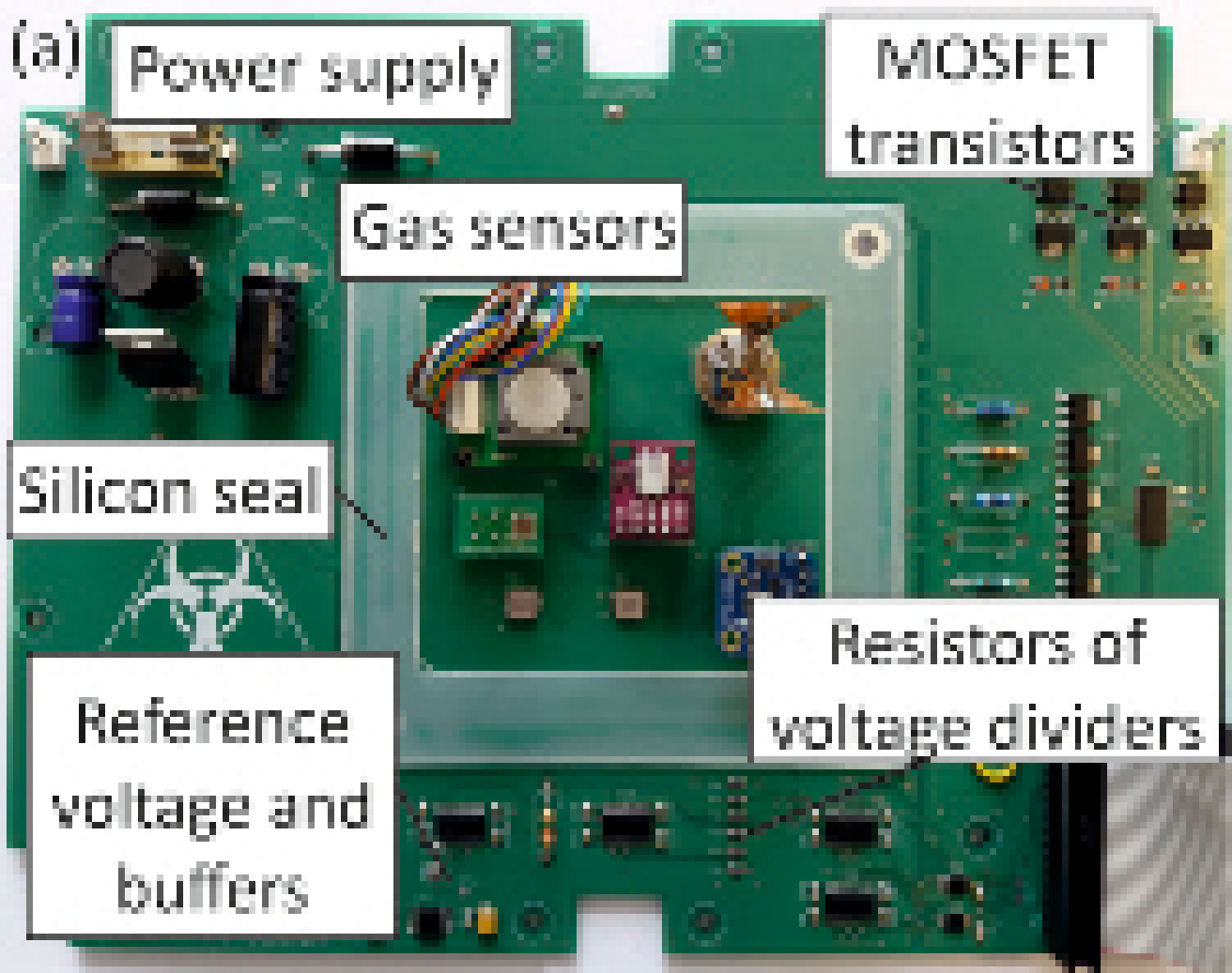
(a)
Power supply
MOSFET transistors
Gas sensors
Silicon seal
Resistors of voltage dividers
Reference voltage and buffers

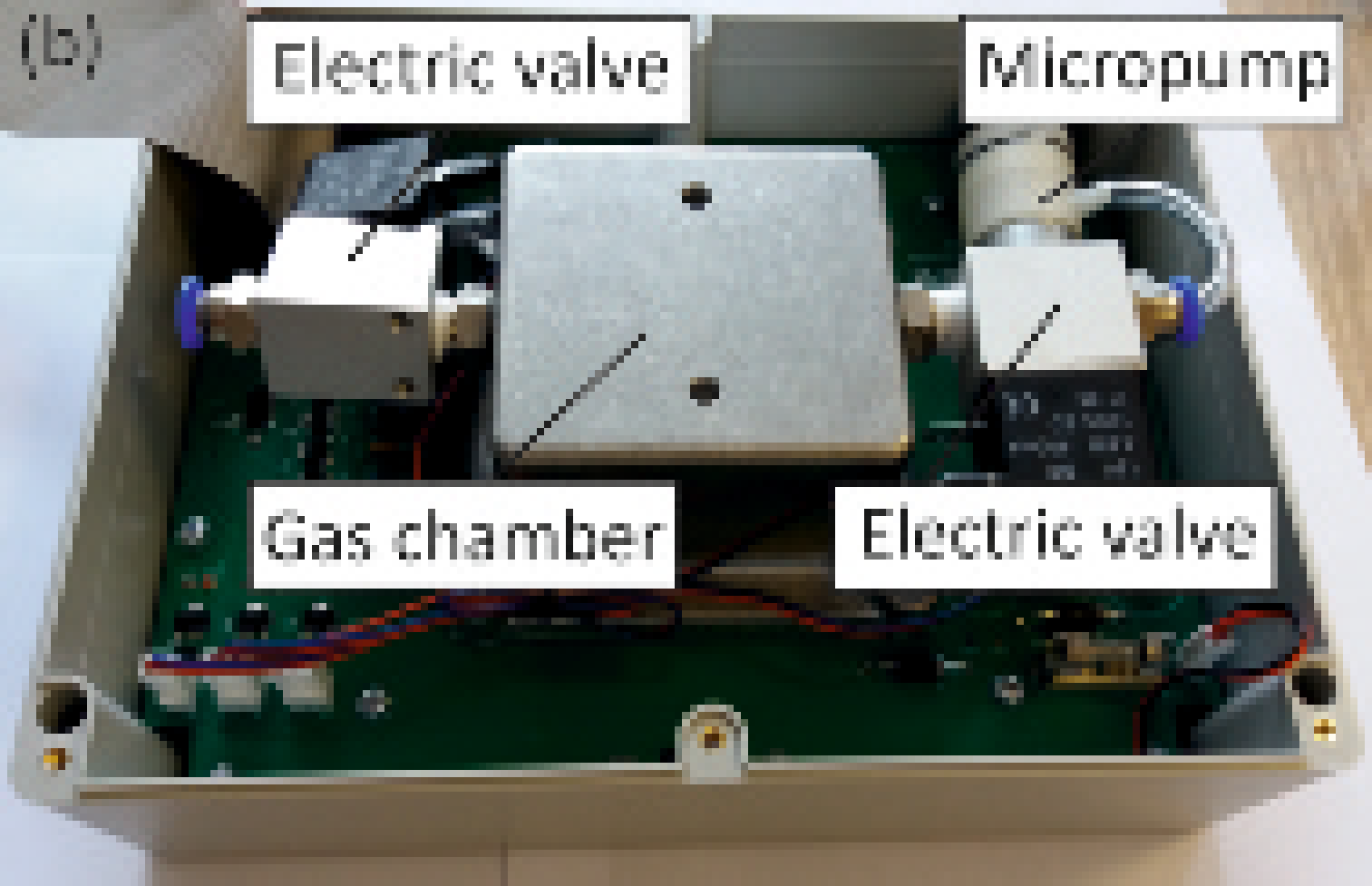
(b)
Electric valve
Micropump
Gas chamber
Electric valve

(c)

Embedded control unit
M5Stack Core2 ESP32 IoT

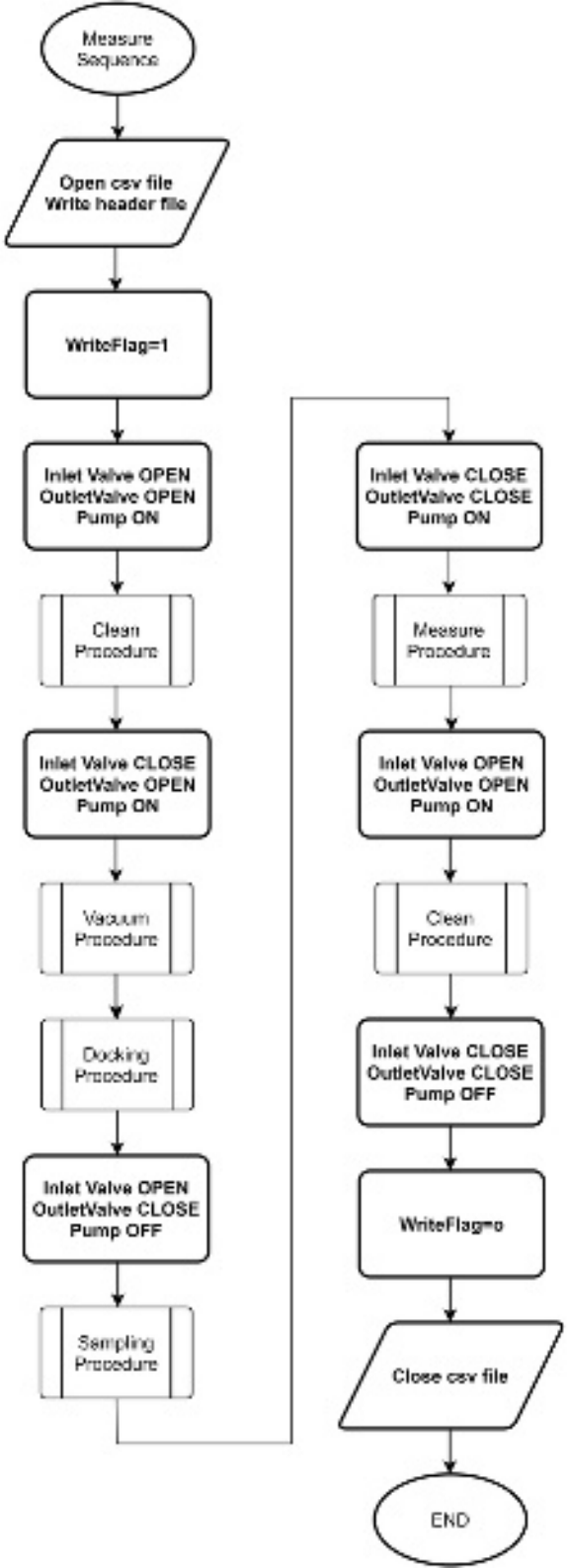
Measure Sequence
Open csv file
Write header file
WriteFlag=1
Inlet Valve OPEN
OutletValve OPEN
Pump ON
Clean Procedure
Inlet Valve CLOSE
OutletValve OPEN
Pump ON
Vacuum Procedure
Docking Procedure
Inlet Valve OPEN
OutletValve CLOSE
Pump OFF
Sampling Procedure
Inlet Valve CLOSE
OutletValve CLOSE
Pump ON
Measure Procedure
Inlet Valve OPEN
OutletValve OPEN
Pump ON
Clean Procedure
Inlet Valve CLOSE
OutletValve CLOSE
Pump OFF
WriteFlag=0
Close csv file
END

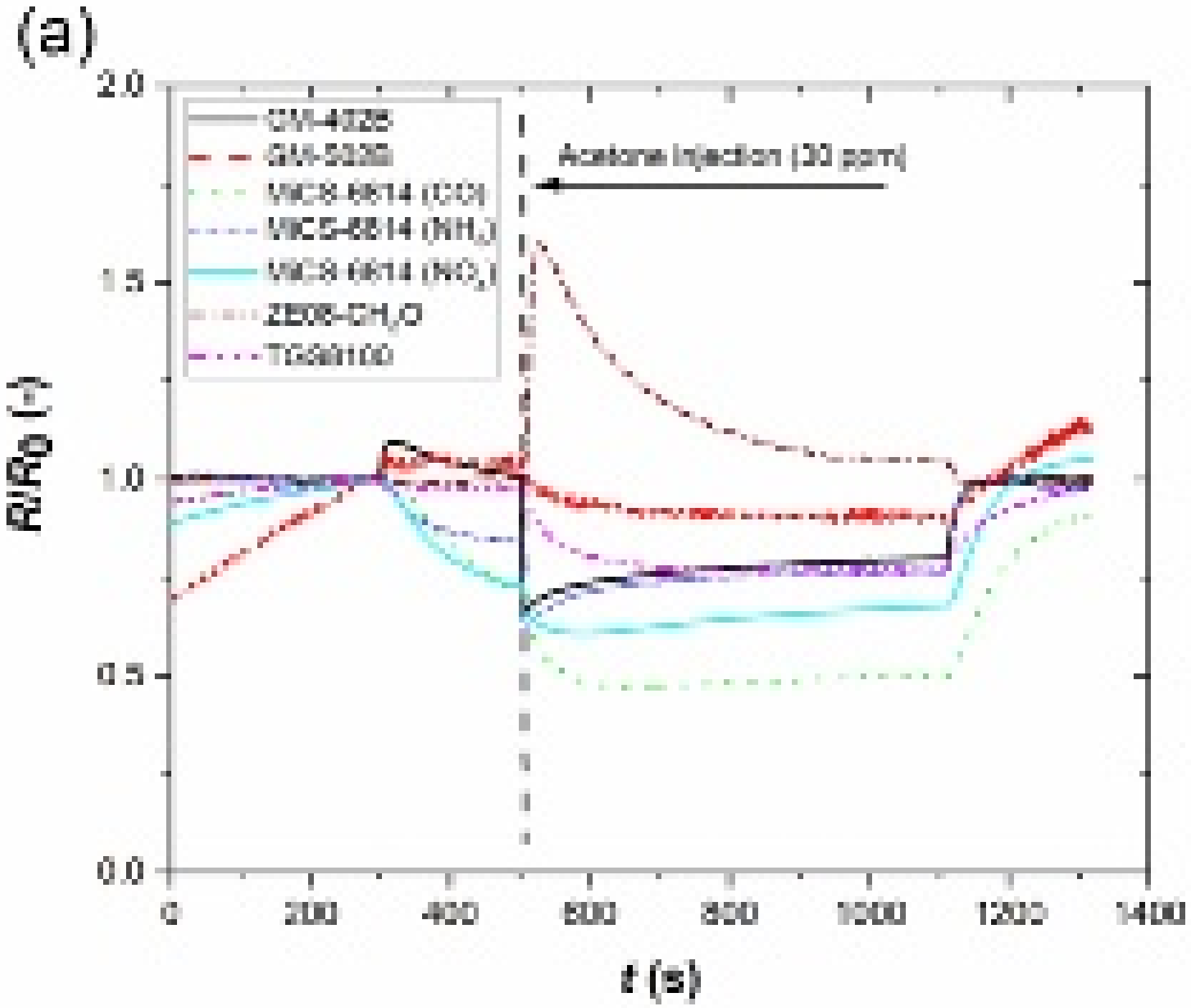
(a)
2.0
1.5
1.0
0.5
0.0
R/R0 (-)
0
200
400
600
800
1000
1200
1400
t (s)
Acetone injection (30 ppm)
GM-4328
GM-5328
VICS-6614 (CO)
VICS-6614 (NH3)
VICS-6614 (NO2)
ZE08-CH2O
TGS8100

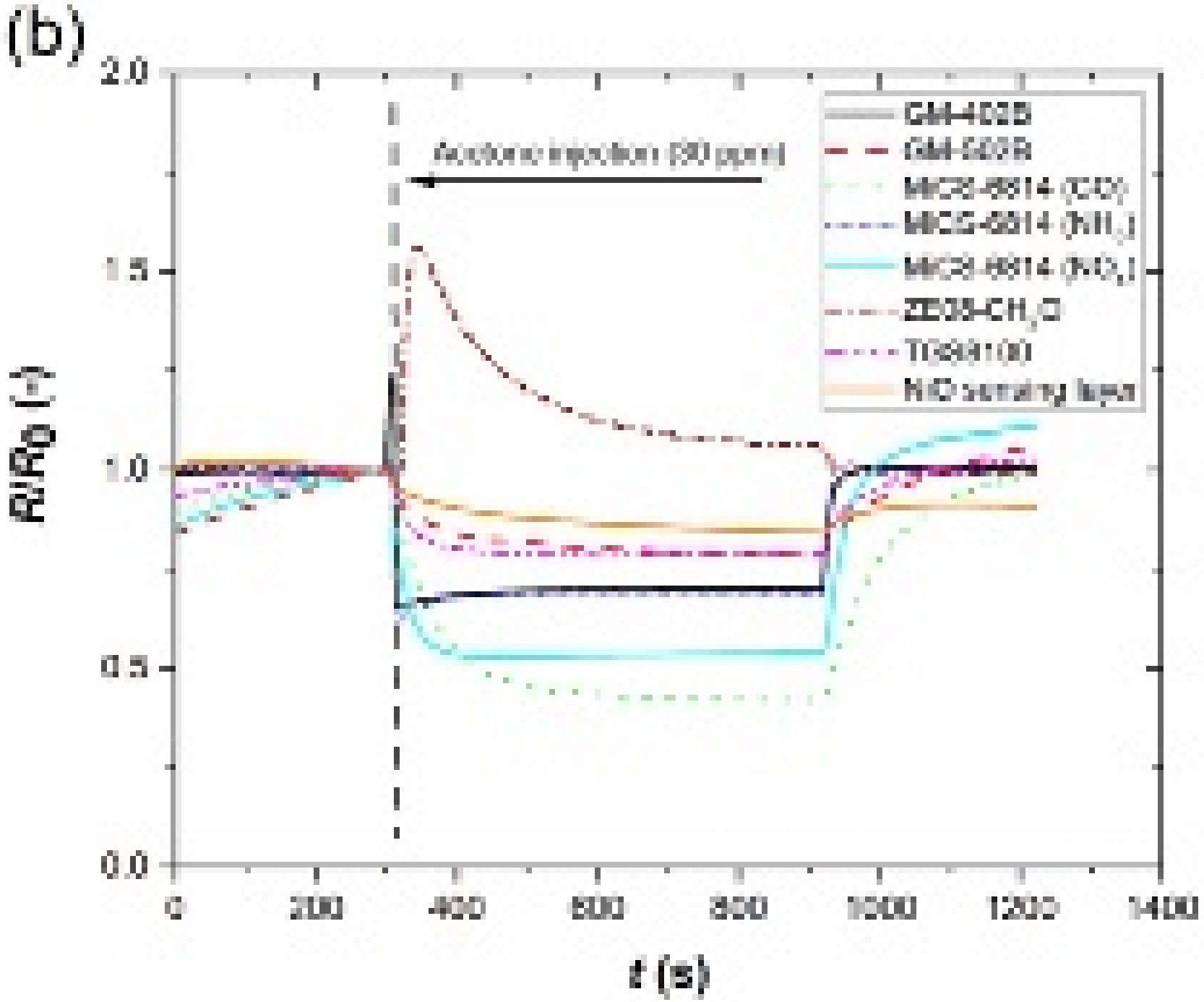
(b)
2.0
1.5
1.0
0.5
0.0
R/R0 (-)
Acetone injection (50 ppm)
GM-402B
GM-502B
MICS-6814 (CO)
MICS-6814 (NH3)
MICS-6814 (NO2)
ZE03-CH2O
TGS8100
NiO sensing layer
0
200
400
600
800
1000
1200
1400
t (s)

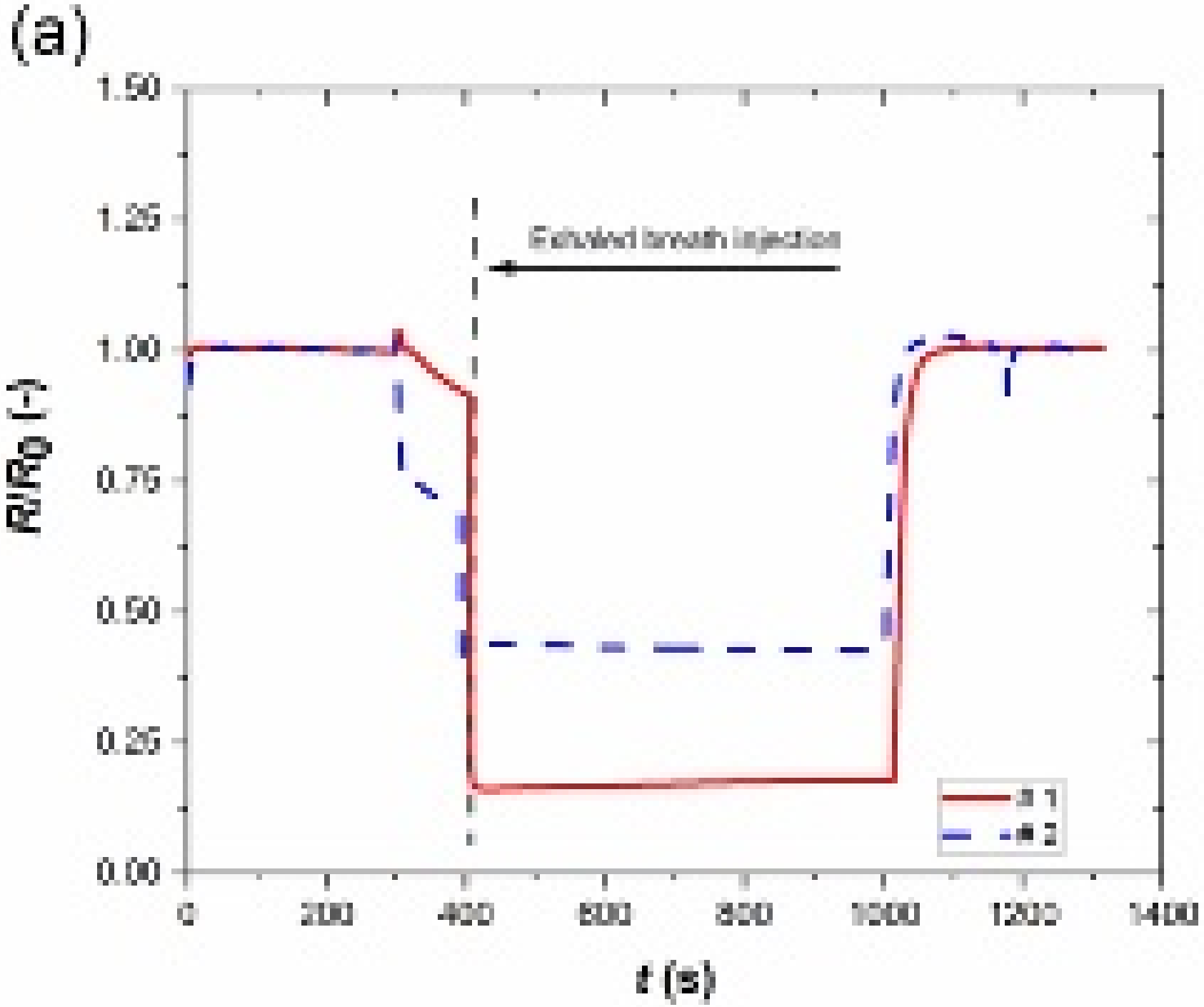
(a)
1.50
1.25
1.00
0.75
0.50
0.25
0.00
R/R0 (-)
0
200
400
600
800
1000
1200
1400
t (s)

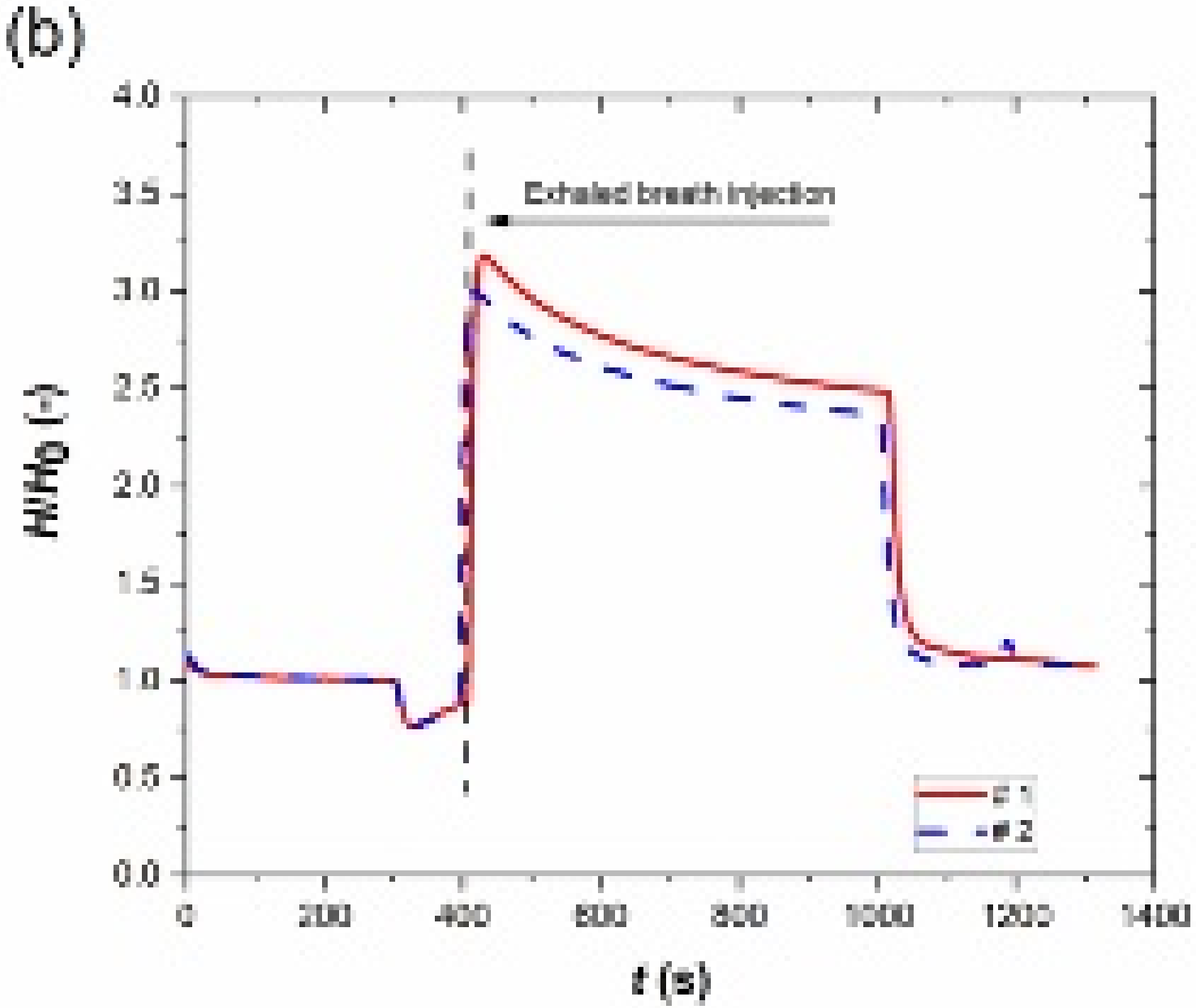
(b)
Exhaled breath injection
R/R0 (-)
t (s)
#1
#2

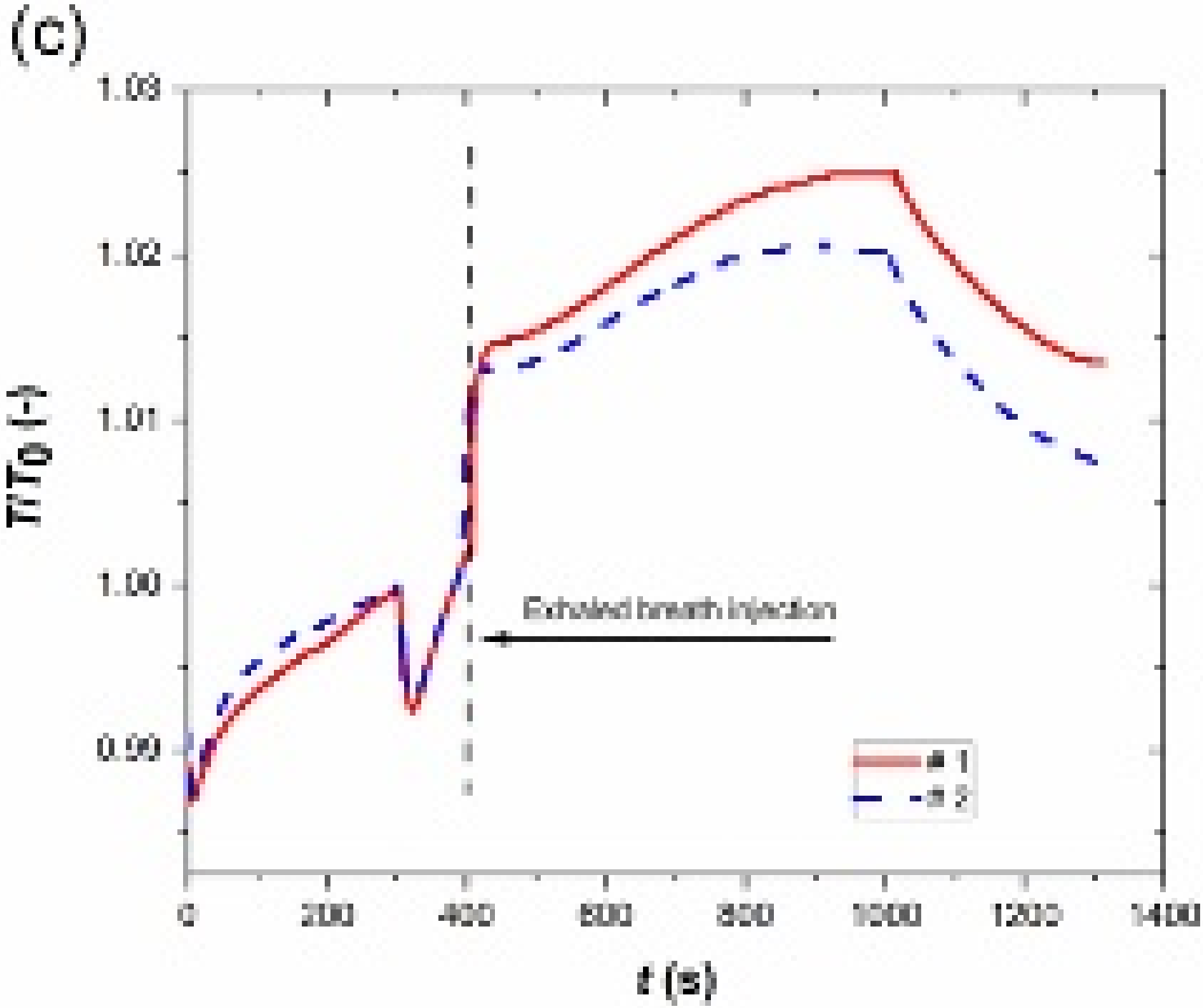
(c)
1.03
1.02
1.01
1.00
0.99
T/T0 (-)
Exhaled breath injection
0
200
400
600
800
1000
1200
1400
t (s)

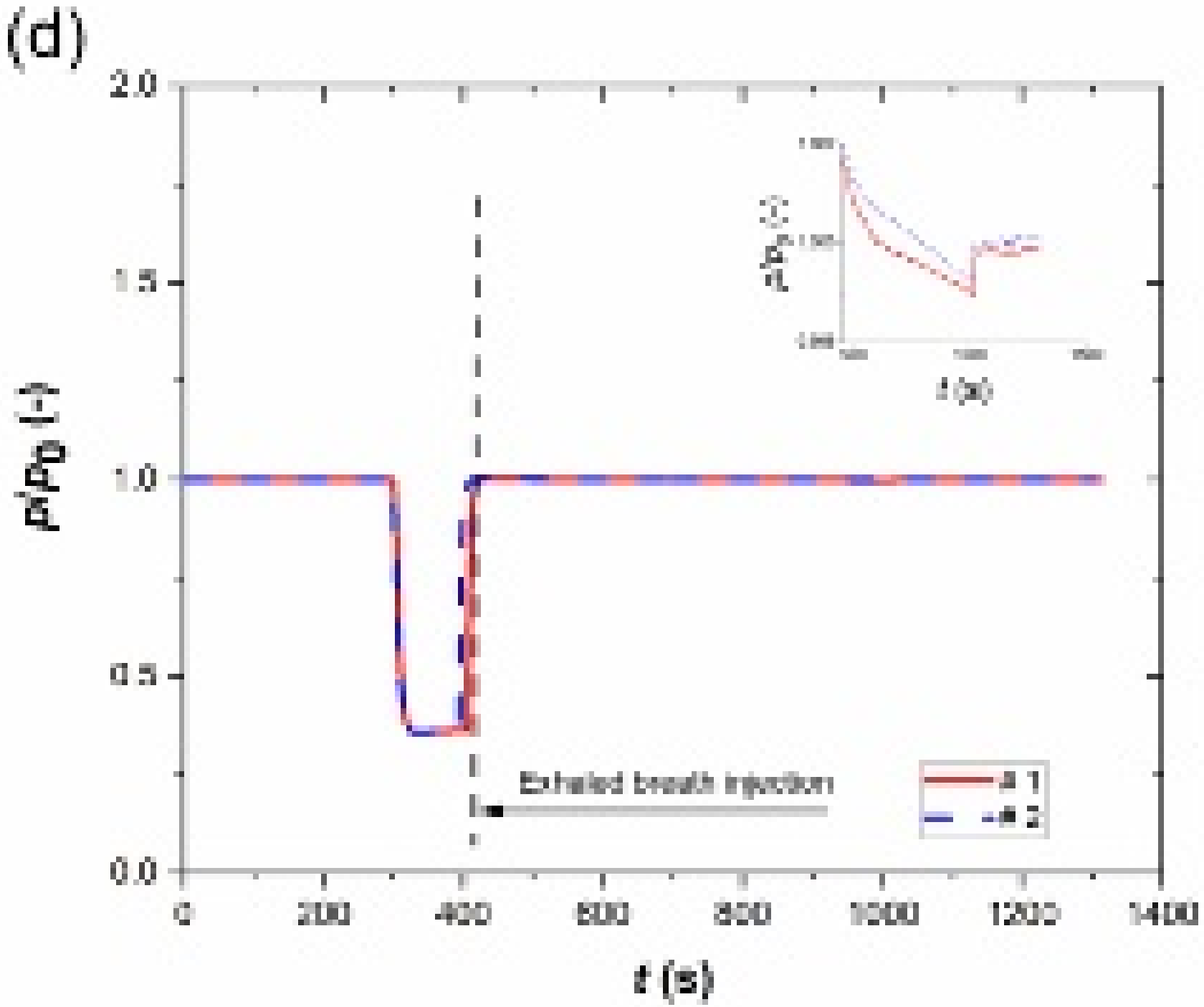
(d)
2.0
1.5
1.0
0.5
0.0
0
200
400
600
800
1000
1200
1400
p'/p0 (-)
t (s)
Exhaled breath injection
1
2